

Supporting Information

Visible-light Photocatalytic, Solar Thermal and Photoelectrochemical Properties of Aluminium-reduced Black Titania

*Zhou Wang,^{a,b} Chongyin Yang,^{a,b} Tianquan Lin,^{a,b} Hao Yin,^a Ping Chen,^a Dongyun
Wan,^{*a} Fangfang Xu,^a Fuqiang Huang,^{*a,b} Jianhua Lin,^b Xiaoming Xie,^c Mianheng
Jiang^c*

^aCAS Key Laboratory of Materials for Energy Conversion, Shanghai Institute of Ceramics, Chinese Academy of Sciences, Shanghai 200050, China;

^bBeijing National Laboratory for Molecular Sciences, College of Chemistry and Molecular Engineering, Peking University, Beijing 100871, China;

^cState Key Laboratory of Functional Materials for Informatics, Shanghai Institute of Microsystem and Information Technology, Chinese Academy of Sciences, Shanghai 200050, China.

Synthesis

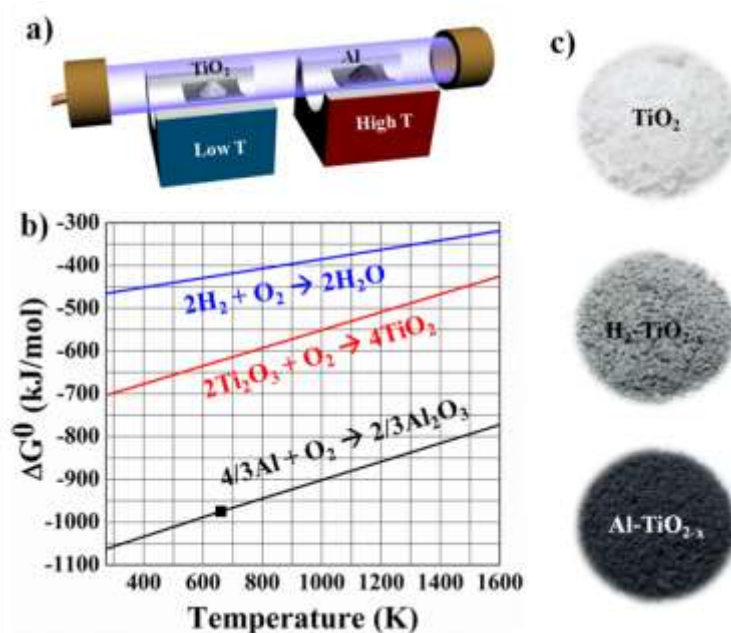


Figure S1. (a) Schematic low-temperature reduction of TiO₂ in a two-zone furnace. (b) Ellingham diagram of ΔG versus temperature. (c) Photographs of pristine TiO₂, gray TiO_{2-x} obtained by H₂ anneal (H₂-TiO_{2-x}), and black TiO_{2-x} obtained by Al reduction (Al-TiO_{2-x}).

The aluminum reduction process for preparing black titania is illustrated in Figure S1a. The reduction process combines the merit of the low/high-temperature compartments, where the reductant (aluminum) is melted in the high-temperature compartment and the reduction is carried out in the low-temperature compartment. This controllable reduction is a thermodynamic and kinetic basis of the two-compartment method, which has been used by us to reduce graphene oxide at 100 – 200 °C.^[S1] From an engineering viewpoint, this configuration allows separate control. Thermodynamically, the reaction driving force enables aluminum oxidation and titania reduction, as the Ellingham diagram is shown in Figure S1b. The straight

lines represent the Gibbs free energy $\Delta G^0(T)$ at different temperature, which indicates the relative stability of oxides. It is possible to visualize directly the affinities of metals for oxygen in their standard conditions by observing the relative positions of their lines in the diagram. A given metal can reduce the oxides of all other metals whose lines lie above others in the diagram. For example, the $2\text{Ti}_2\text{O}_3 + \text{O}_2 \rightarrow 4\text{TiO}_2$ line lies above $4/3\text{Al} + \text{O}_2 \rightarrow 2/3\text{Al}_2\text{O}_3$ line but below the $2\text{H}_2 + \text{O}_2 \rightarrow 2\text{H}_2\text{O}$ line, so elemental Al can reduce TiO_2 to Ti_2O_3 but H_2 cannot reduce TiO_2 at low temperature. This explains why the H_2 gas hardly reduces crystalline TiO_2 below 600 °C.

It is convenient to obtain the equilibrium oxygen partial pressure at a given temperature using the following equation:

$$\Delta G^0 = -RT \ln p_{\text{O}_2}$$

where T is the temperature of the system and p_{O_2} is partial pressure of oxygen. Any combination of values $(\Delta G^0, T)$ in the diagram represents a particular value of equilibrium oxygen partial pressure. If the system oxygen partial pressure is higher than the equilibrium value, the metal will be oxidized, and if it is lower than the equilibrium value then the oxide will be reduced. In this study, the melted Al at 800 °C can effectively decrease the system oxygen partial pressure to a degree much lower than the equilibrium value of TiO_2 , making it easily be reduced.

Sample characterizations:

The optical absorption spectra of samples were obtained at room temperature by the UV-Vis-NIR spectrometer (Hitachi U4100) equipped with an integrating sphere.

Raman spectra were collected on a Thermal Dispersive Spectrometer using a laser with an excitation wavelength of 532 nm at laser power of 10 mW. XPS experiments were carried out on a RBD upgraded PHI-5000C ESCA system (Perkin Elmer) with Mg K α radiation ($h\nu = 1253.6$ eV). The EPR spectra were collected using a Bruker EMX-8 spectrometer at 9.44 GHz at 300 K. The magnetic performance was conducted by a Physical Property Measurement System (PPMS, Quantum Design Company). XRD patterns were obtained with a Bruker D8 advance diffractometer operating with Cu K α radiation. The total organic carbon (TOC) concentration was determined with a TOC analyzer (TOC-VCPH, Shimadzu Corporation, Japan).

Table S1. Proportion of light absorption in different spectrum region.

Sample	Total absorption	UV (<400nm)	Visible (400-760nm)	Infrared (>760nm)
solar spectrum	100%	7%	50%	43%
pristine TiO ₂	5%	5%	0	0
500°C-Al-TiO _{2-x}	65%	5%	32%	28%
HP-TiO ₂	30%	5%	24%	1%

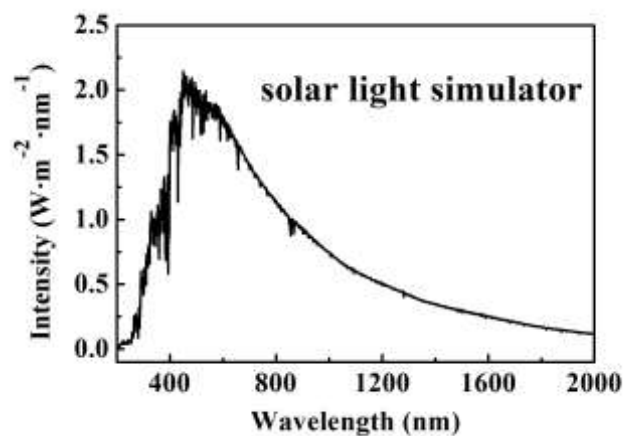


Fig. S2 Emission spectrum of the solar light simulator.

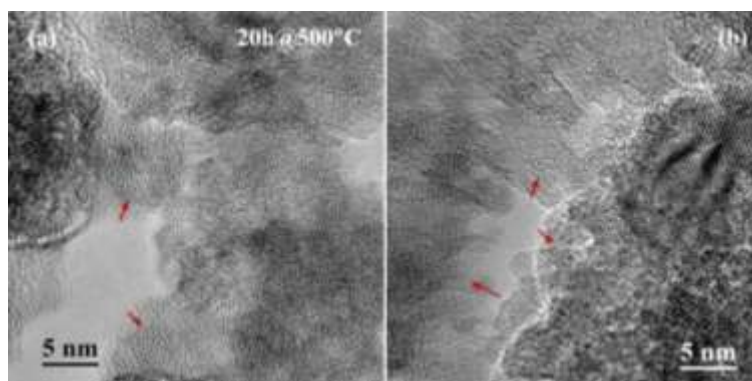


Fig. S3 HRTEM images of TiO_{2-x} prepared by Al-reduction at 500 °C for 20 h. The crystal structure was destroyed when prolonging the Al-reduction time to 20 h.

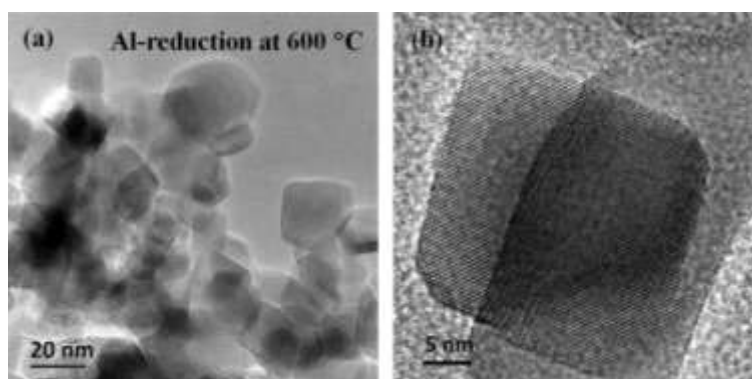


Fig. S4 TEM images of titania prepared by Al-reduced at 600 °C for 6 h. The amorphous shell vanished by recrystallization under this reduction condition.

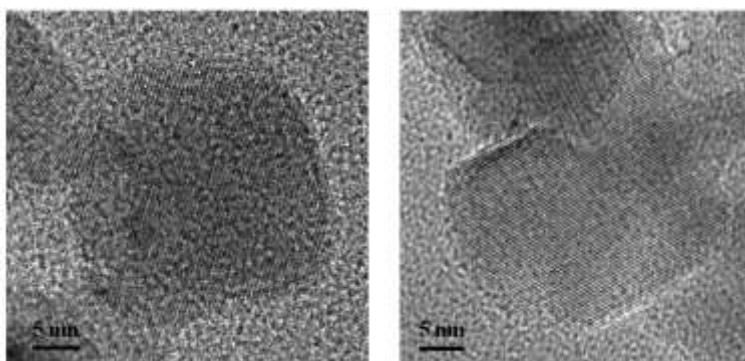


Fig. S5 HRTEM images of titania reduced by H₂ under atmosphere pressure. The nanocrystals keep high crystallinity without amorphous layer on the surface.

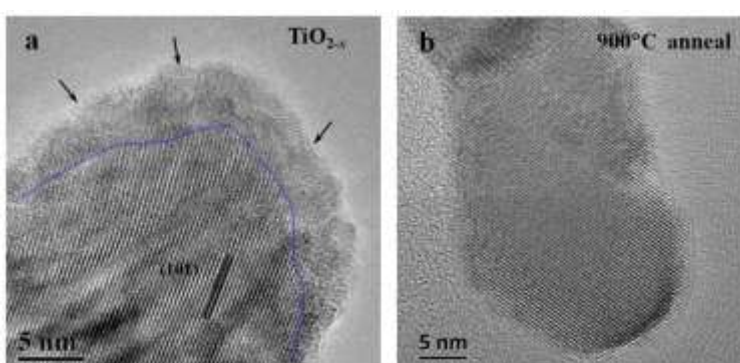


Fig. S6 (a, b) HRTEM images of TiO_{2-x} and after heat treatment at 900 °C for 12 h, respectively.



Fig. S7 (a) Photographs of black TiO_{2-x} and after heat treatment at 800 °C and 900 °C for 12 h in Ar atmosphere, respectively. The coloration of the sample turned from black to gray (800 °C) to white (900 °C).

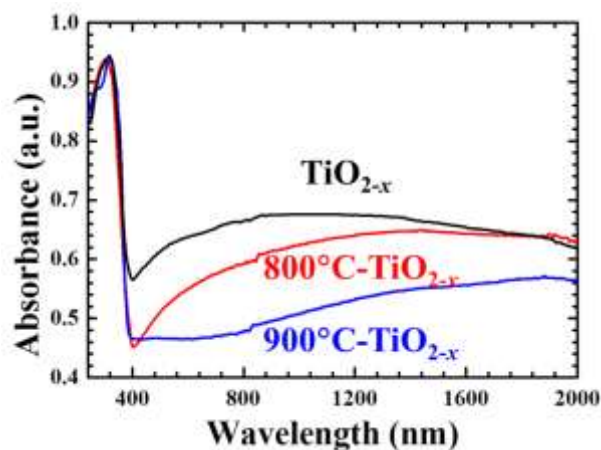


Fig. S8 UV-vis-IR absorption spectra of the 500°C-reduced black TiO_{2-x} before and after annealing at 800 °C and 900 °C in Ar atmosphere.

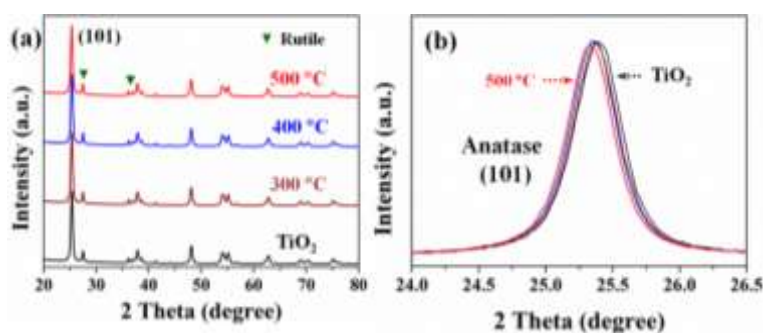


Fig. S9 (a) XRD patterns of TiO₂ before and after the Al reduction at different temperatures for 6 h. The strong XRD diffraction peaks indicated that the pristine TiO₂ and black TiO_{2-x} are highly crystalline with a mixture of anatase and rutile. Nevertheless, black TiO_{2-x} exhibits a larger linewidth than pristine TiO₂ shown in (b).

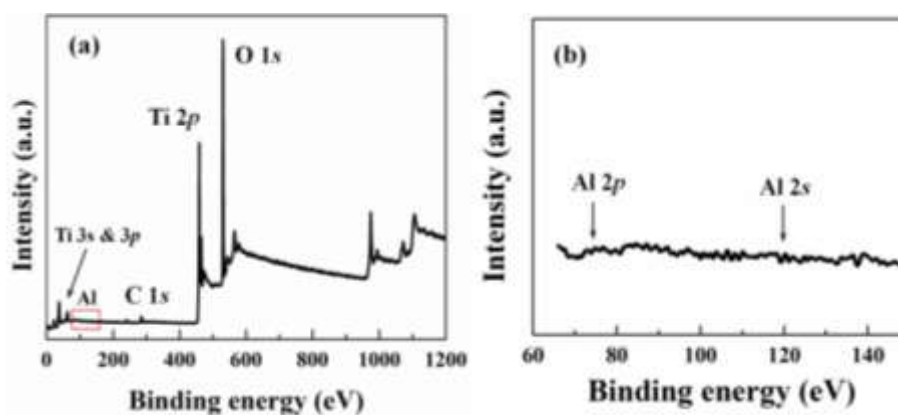


Fig. S10 XPS survey spectra of black TiO_{2-x} obtained at 500 °C.

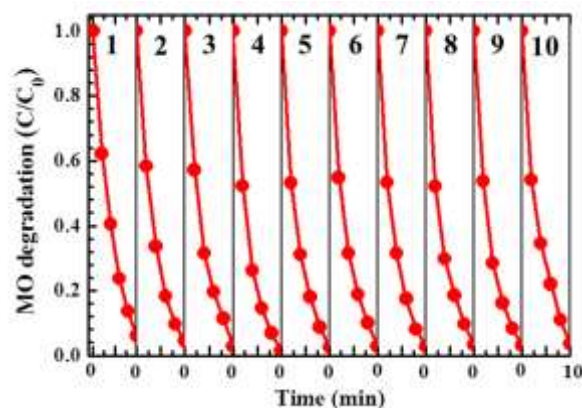


Fig. S11 Cycling degradation of methylene orange over the 500°C-reduced black TiO_{2-x} .

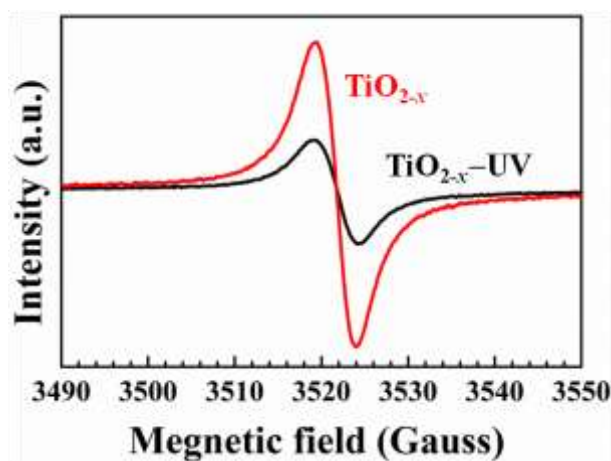


Fig. S12 EPR spectra of black titania samples before and after UV-light irradiation in water for 30 min are denoted as TiO_{2-x} and TiO_{2-x} -UV, respectively.

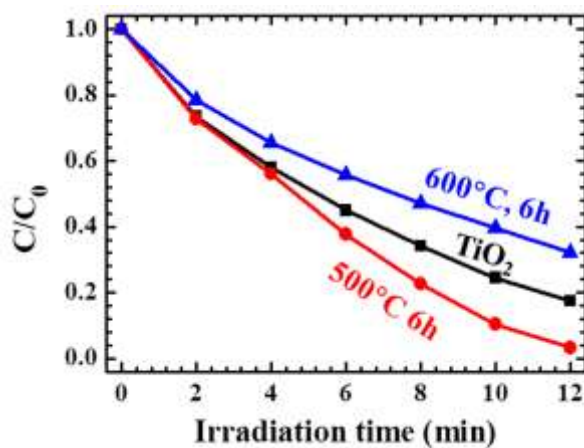


Fig. S13 Photocatalytic decomposition of methyl orange. The TiO_{2-x} with core/shell structure ($\text{TiO}_2@\text{TiO}_{2-x}$) possesses the highest photocatalytic activities confirming that the unique structure has the key role to play in the photocatalysis.

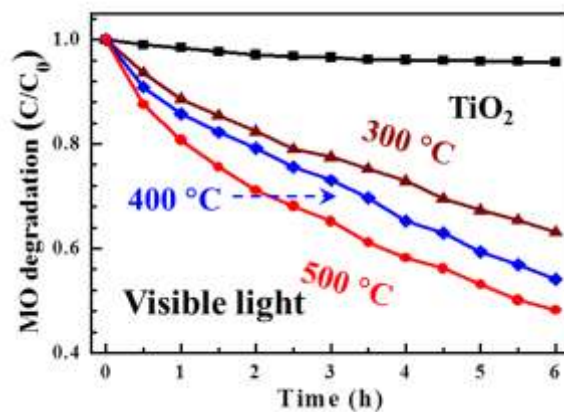


Fig. S14 Visible light photocatalytic degradation of methyl orange.

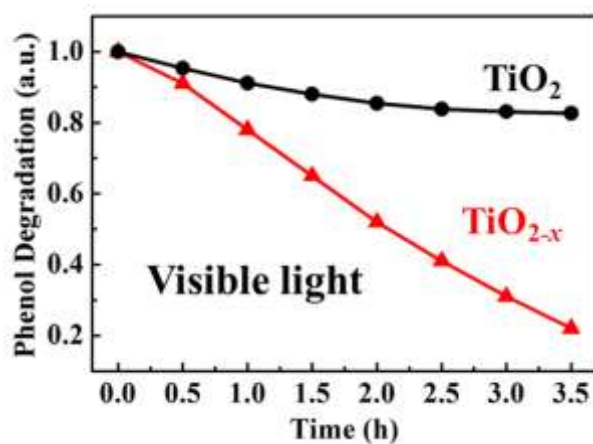


Fig. S15 Photocatalytic degradation of phenol under visible-light irradiation.

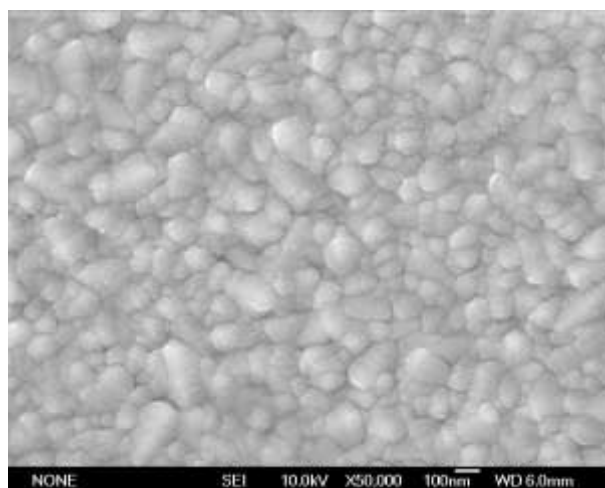


Fig. S16 FESEM image of Al-reduced TiO_{2-x} film (top morphology).

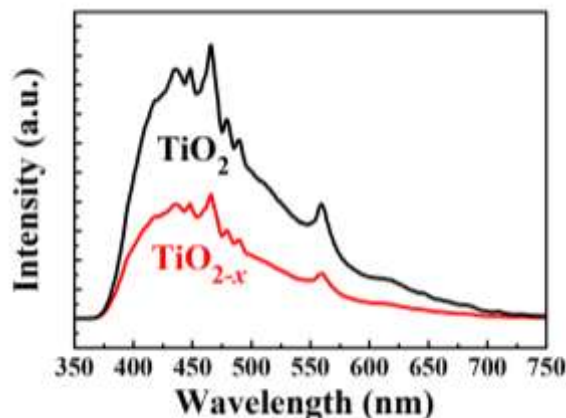


Fig. S17 PL spectra of 500°C-reduced TiO_{2-x} and pristine titania (TiO_2)

Computational details

The density-functional theory (DFT) computations have been implemented in the Vienna Ab initio Simulation Package (VASP).^[S2,3] The Perdew-Burke-Ernzerhof (PBE)^[S4] version of the generalized gradient approximation (GGA) is used to describe the exchange correlation functional and the projector augmented wave^[S5] (PAW) method has been used in the present work. The model was constructed on the 1×1 (101) surface (30 atomic layer) with a 20 Å vacuum layer. Here, the cutoff energy of plane wave was chosen at 450 eV. For the structure optimizations, $7 \times 10 \times 1$ Monkhorst-Pack (MP) grids were used. The relaxation of geometry optimization was performed until the total energy changes within 10^{-5} eV/atom and the Hellmann-Feynman force on all atomic sites was less than 0.05 eV /Å.

References

- [S1] D. Wan, C. Yang, T. Lin, Y. Tang, M. Zhou, Y. Zhong, F. Huang, J. Lin, *ACS Nano*, **2012**, 6, 9068.
- [S2] G. Kresse, J. Furthmüller, *Comp. Mater. Sci.*, **1996**, 6, 15-50.
- [S3] G. Kresse, J. Furthmüller, *Phys. Rev. B*, **1996**, 54, 11169.
- [S4] J. P. Perdew, K. Burke, M. Ernzerhof, *Phys. Rev. Lett.*, **1996**, 77, 3865-3868.
- [S5] P. E. Blöchl, *Phys. Rev. B*, **1994**, 50, 17953- 17979.